Eur. Phys. J. C (2022) 82:148
https://doi.org/10.1140/epjc/s10052-021-09903-1

THE EUROPEAN PHYSICAL JOURNAL C

Regular Article - Theoretical Physics

Higgs triplet extension of GRACE

Yusaku Kouda[1,a], **Tadashi Kon**[1,b], **Yoshimasa Kurihara**[2,c], **Takahiro Ueda**[1,d]

[1] Faculty of Science and Technology, Seikei University, 3-3-1 Kichijoji-Kitamachi, Musashino, Tokyo 180-8633, Japan
[2] High Energy Accelerator Organization (KEK), Tsukuba, Ibaraki 305-0801, Japan

Received: 20 October 2021 / Accepted: 2 December 2021 / Published online: 16 February 2022

Abstract Much theoretical effort and automatization are required to confront new physics models with experimental data for many types of particle reactions at future colliders. In this context, we extend GRACE, an automatic calculation system for invariant amplitudes, to incorporate particles and interactions in the Georgi–Machacek model. With the extended GRACE system, we study fermiophobic Higgs boson production processes at e^+e^- and e^-e^- colliders in the model. The results show some advantages of e^-e^- colliders over e^+e^- colliders for new physics search and thus its complementary role.

1 Introduction

The discovery of a Higgs boson in 2012 [1,2] completed the last piece missing from the Standard Model (SM) of particle physics. Nevertheless, there is still much that cannot be explained within the SM. Some of the open questions are addressed by extending the Higgs sector or by models that force us to extend that sector (see Refs. [3,4] for recent reviews on models with extended Higgs sectors). Vast possibilities for non-minimal Higgs sectors will be tested by comparing future experimental data with model predictions. To obtain a quantitative prediction for the collider phenomenology, one may use tools dedicated to specific models (e.g., [5,6]) or general-purpose tools written in a model-independent way (see Ref. [7] and references therein).

The aim of this paper is twofold. Firstly, we discuss extending the public version of the GRACE system [8–10] for models with exotic Higgs particles, beyond isospin doublets. Here, we focus on the Georgi–Machacek (GM) model [11] as a concrete example that contains isospin triplets while keeping the custodial symmetry naturally [12] and has rich collider phenomenology, e.g., [13–15]. In fact, one can implement a new model with GRACE by preparing a set of files describing the model, i.e., particle contents, interaction vertices, model parameters, etc. Once the model files are established, then in principle one can compute any tree-level decay and scattering amplitudes.

Secondly, using GRACE equipped with the GM model, we compute production cross sections of fermiophobic custodial 5-plet Higgs bosons ($H_5^{\pm\pm}$, $H_5^{\pm}$, H_5^0) at future e^+e^- and e^-e^- colliders. It is known that a clear signature of physics beyond the SM at e^-e^- colliders may come from W^-W^- production [16,17], which is the counterpart of the same-sign $W^\pm W^\pm$ production measurement at the LHC [18,19]. Notably, Ref. [17] considered the resonant effect of H_5^{--} on W^-W^- production cross section at e^-e^- colliders in the GM model. See Ref. [20] for other physics cases at e^-e^- colliders. Comparing the production cross sections in e^+e^- collisions [13,15] with those in e^-e^- collisions, we will see advantages of the latter for the 5-plet Higgs boson search.

The GM model adds isospin triplets in the scalar sector, the vacuum expectation values (VEVs) of which could give raise to Majorana neutrino masses by the type-II seesaw mechanism [21–25] as other Higgs triplet models, while naturally maintaining the electroweak ρ parameter as unity at the tree level.[1] Higgs bosons in the same custodial multiplet have degenerated masses at the tree level [12,14], which may make the model easily distinguishable from other models. The SM-like Higgs boson's couplings to the weak gauge bosons can be larger than those in the SM [27], which is favored by the slightly larger central values measured by the ATLAS experiment [28] (but see also the CMS result [29]). The model allows the strong first-order electroweak phase transition [30,31], thus provides a scenario of electroweak baryogenesis. Theoretical constraints on the

[a] e-mail: s91661@cc.seikei.ac.jp
[b] e-mail: kon@st.seikei.ac.jp
[c] e-mail: kurihara@post.kek.jp (corresponding author)
[d] e-mail: tueda@st.seikei.ac.jp

[1] See, however, Ref. [26] for ρ at the one-loop level.

parameter space in the GM model are examined in Refs. [32–35]. See Refs. [36–40] for recent experimental constraints and parameter space analyses.

This paper is organized as follows. In Sect. 2, we give the definition of the GM model to clarify our conventions. In Sect. 3, we discuss an extension of the GRACE system to the GM model. Numerical results for custodial 5-plet Higgs boson production cross sections are shown in Sec. 4, which exhibit some advantages of e^-e^- colliders over e^+e^- colliders for new physics searches. Section 5 is devoted to the summary.

2 Model

Here, we briefly recapitulate the GM model [11] with the focus on the physical Higgs bosons.[2] The Higgs sector of the GM model contains one real isospin triplet field ξ with hypercharge $Y = 0$ and one complex isospin triplet field χ with $Y = 1$, as well as the usual complex isospin doublet field ϕ with $Y = 1/2$ in the SM. It is convenient to express these scalar fields as $SU(2)_L \times SU(2)_R$ bi-doublet and bi-triplet:

$$\Phi = \begin{pmatrix} (\phi^0)^* & \phi^+ \\ -(\phi^+)^* & \phi^0 \end{pmatrix}, \quad \Delta = \begin{pmatrix} (\chi^0)^* & \xi^+ & \chi^{++} \\ -(\chi^+)^* & \xi^0 & \chi^+ \\ (\chi^{++})^* & -(\xi^+)^* & \chi^0 \end{pmatrix}. \tag{2.1}$$

The kinetic terms for the scalar fields are given as

$$\mathcal{L}_{\rm kin} = \frac{1}{2}\,\mathrm{tr}\left[(\mathcal{D}_\mu\Phi)^\dagger(\mathcal{D}^\mu\Phi)\right] + \frac{1}{2}\,\mathrm{tr}\left[(\mathcal{D}_\mu\Delta)^\dagger(\mathcal{D}^\mu\Delta)\right], \tag{2.2}$$

where the covariant derivatives are defined by

$$\mathcal{D}_\mu\Phi = \partial_\mu\Phi + ig\frac{\tau^a}{2}W^a_\mu\Phi - ig'B_\mu\Phi\frac{\tau^3}{2}, \tag{2.3}$$

$$\mathcal{D}_\mu\Delta = \partial_\mu\Delta + igt^aW^a_\mu\Delta - ig'B_\mu\Delta t^3, \tag{2.4}$$

with τ^a being the Pauli matrices and t^a being generators for $SU(2)$ triplet representations, which one can choose

$$t^1 = \frac{1}{\sqrt{2}}\begin{pmatrix} 0&1&0\\1&0&1\\0&1&0\end{pmatrix}, \quad t^2 = \frac{1}{\sqrt{2}}\begin{pmatrix} 0&-i&0\\i&0&-i\\0&i&0\end{pmatrix},$$
$$t^3 = \begin{pmatrix} 1&0&0\\0&0&0\\0&0&-1\end{pmatrix}. \tag{2.5}$$

The most general Higgs potential preserving the $SU(2)_L \times SU(2)_R$ symmetry [32] is given in our conventions as

$$\begin{aligned} V_H =\ & m_1^2\,\mathrm{tr}(\Phi^\dagger\Phi) + m_2^2\,\mathrm{tr}(\Delta^\dagger\Delta) + \lambda_1\left[\mathrm{tr}(\Phi^\dagger\Phi)\right]^2 \\ & + \lambda_2\left[\mathrm{tr}(\Delta^\dagger\Delta)\right]^2 \\ & + \lambda_3\,\mathrm{tr}\left[(\Delta^\dagger\Delta)^2\right] + \lambda_4\,\mathrm{tr}(\Phi^\dagger\Phi)\,\mathrm{tr}(\Delta^\dagger\Delta) \\ & + \lambda_5\,\mathrm{tr}\left(\Phi^\dagger\frac{\tau^a}{2}\Phi\frac{\tau^b}{2}\right)\mathrm{tr}(\Delta^\dagger t^a\Delta t^b) \\ & + \mu_1\,\mathrm{tr}\left(\Phi^\dagger\frac{\tau^a}{2}\Phi\frac{\tau^b}{2}\right)(P^\dagger\Delta P)^{ab} \\ & + \mu_2\,\mathrm{tr}(\Delta^\dagger t^a\Delta t^b)(P^\dagger\Delta P)^{ab}, \end{aligned} \tag{2.6}$$

where the matrix P is defined as

$$P = \begin{pmatrix} -\frac{1}{\sqrt{2}} & \frac{i}{\sqrt{2}} & 0 \\ 0 & 0 & 1 \\ \frac{1}{\sqrt{2}} & \frac{i}{\sqrt{2}} & 0 \end{pmatrix}. \tag{2.7}$$

Note that if one sets both the trilinear couplings μ_1 and μ_2 to zero, which leads to the conventional $\mathbb{Z}_2$ symmetric version of the GM model [12], then the model is already highly constrained [41].

The spontaneous symmetry breaking is triggered by the VEVs of the neutral components of the scalar fields:

$$\langle\Phi\rangle = \frac{v_\phi}{\sqrt{2}}\begin{pmatrix}1&0\\0&1\end{pmatrix}, \quad \langle\Delta\rangle = v_\Delta\begin{pmatrix}1&0&0\\0&1&0\\0&0&1\end{pmatrix}. \tag{2.8}$$

The weak bosons acquire their masses as

$$m_W^2 = m_Z^2\cos^2\theta_W = \frac{g^2}{4}v^2, \tag{2.9}$$

where $v^2 = 1/(\sqrt{2}G_F) \approx (246\,\mathrm{GeV})^2$ consists of contributions from the two VEVs:

$$v^2 = v_\phi^2 + 8v_\Delta^2. \tag{2.10}$$

We define the doublet-triplet mixing angle θ_H as $\tan\theta_H = 2\sqrt{2}v_\Delta/v_\phi$, and use abbreviations $s_H = \sin\theta_H$, $c_H = \cos\theta_H$ and $t_H = \tan\theta_H$. The minimization conditions of

[2] Our conventions are almost the same as those in Ref. [14] except that we do not introduce M_1^2 and M_2^2 in Eq. (2.9) of Ref. [14] and we use $(\chi^{++})^*$, $(\xi^+)^*$, $(\phi^+)^*$, etc. in this section rather than χ^{--}, ξ^-, ϕ^-, etc. Note that there are many conventions used in the literature for the parameterization of the Higgs potential, (signs of) mixing angles and so on.

the Higgs potential relate the VEVs to the other dimensionful parameters in the potential, which allows one to eliminate m_1^2 and m_2^2. Note that the VEVs of the neutral components of the triplet fields are taken to be the same value, $\langle \xi^0 \rangle = \langle \chi^0 \rangle = v_\Delta$. This preserves the diagonal custodial $SU(2)_V$ symmetry after its spontaneous breaking $SU(2)_L \times SU(2)_R \to SU(2)_V$ and keeps the electroweak ρ parameter, $\rho \equiv m_W^2/(m_Z^2 \cos^2\theta_W)$, as unity at the tree level.

Given the exact form of the Higgs potential and the symmetry breaking pattern, one can determine the relations between the weak eigenstates and the mass eigenstates of the scalar fields. The preserved custodial symmetry classifies the states as $SU(2)_V$ multiplets; the field Φ contains a 3-plet and a singlet while the field Δ contains a 5-plet, a 3-plet and a singlet. In general, the two 3-plets coming from Φ and Δ mix each other. The same happens for the two singlets. Consequently, the components fields in Φ and Δ are related to physical Higgs boson states (H_5^{++}, H_5^+, H_5^0), (H_3^+, H_3^0), H_1^0, h and Nambu–Goldstone boson states (G^+, G^0) as follows:

$$\chi^{++} = H_5^{++}, \tag{2.11}$$

$$\begin{pmatrix} \phi^+ \\ \xi^+ \\ \chi^+ \end{pmatrix} = \begin{pmatrix} 1 & 0 & 0 \\ 0 & \frac{1}{\sqrt{2}} & -\frac{1}{\sqrt{2}} \\ 0 & \frac{1}{\sqrt{2}} & \frac{1}{\sqrt{2}} \end{pmatrix} \begin{pmatrix} c_H & -s_H & 0 \\ s_H & c_H & 0 \\ 0 & 0 & 1 \end{pmatrix} \begin{pmatrix} G^+ \\ H_3^+ \\ H_5^+ \end{pmatrix}, \tag{2.12}$$

$$\begin{pmatrix} \phi_i \\ \chi_i \end{pmatrix} = \begin{pmatrix} c_H & -s_H \\ s_H & c_H \end{pmatrix} \begin{pmatrix} G^0 \\ H_3^0 \end{pmatrix}, \tag{2.13}$$

$$\begin{pmatrix} \phi_r \\ \xi_r \\ \chi_r \end{pmatrix} = \begin{pmatrix} 1 & 0 & 0 \\ 0 & \frac{1}{\sqrt{3}} & -\sqrt{\frac{2}{3}} \\ 0 & \sqrt{\frac{2}{3}} & \frac{1}{\sqrt{3}} \end{pmatrix} \begin{pmatrix} c_\alpha & -s_\alpha & 0 \\ s_\alpha & c_\alpha & 0 \\ 0 & 0 & 1 \end{pmatrix} \begin{pmatrix} h \\ H_1^0 \\ H_5^0 \end{pmatrix}. \tag{2.14}$$

Here, we have parameterized the neutral component fields ϕ^0, χ^0 and ξ_0 as

$$\phi^0 = \frac{1}{\sqrt{2}}(\phi_r + v_\phi + i\phi_i), \quad \chi^0 = \frac{1}{\sqrt{2}}(\chi_r + i\chi_i) + v_\Delta, \quad \xi^0 = \xi_r + v_\Delta. \tag{2.15}$$

Another mixing angle α has been introduced for the $SU(2)_V$ singlet states (via $s_\alpha \equiv \sin\alpha$ and $c_\alpha \equiv \cos\alpha$), which diagonalizes a submatrix

$$M^2_{\substack{\text{CP-even} \\ \text{singlet}}} = \begin{pmatrix} M_{11}^2 & M_{12}^2 \\ M_{12}^2 & M_{22}^2 \end{pmatrix}, \tag{2.16}$$

where

$$M_{11}^2 = 8c_H^2 \lambda_1 v^2, \tag{2.17}$$

$$M_{22}^2 = s_H^2(3\lambda_2 + \lambda_3)v^2 - \frac{1}{\sqrt{2}}\frac{c_H^2}{s_H}\mu_1 v + \frac{3}{\sqrt{2}} s_H \mu_2 v, \tag{2.18}$$

$$M_{12}^2 = \sqrt{\frac{3}{2}} s_H c_H (2\lambda_4 + \lambda_5)v^2 + \frac{\sqrt{3}}{2} c_H \mu_1 v, \tag{2.19}$$

and is determined by

$$\tan 2\alpha = \frac{2M_{12}^2}{M_{11}^2 - M_{22}^2}. \tag{2.20}$$

Without loss of generality, one can choose the state h in such a way that h is lighter than H_1^0 by fixing the sign of α as

$$\mathrm{sgn}(\sin 2\alpha) = -\,\mathrm{sgn}\left(M_{12}^2\right), \tag{2.21}$$

see the mass eigenvalues below. In this paper, we identify the lighter singlet state h as the 125 GeV Higgs boson.

The masses of the physical Higgs boson states are as follows:

$$\begin{aligned} m_{H_5}^2 &\equiv m_{H_5^{++}}^2 = m_{H_5^+}^2 = m_{H_5^0}^2 \\ &= \left(s_H^2 \lambda_3 - \frac{3}{2} c_H^2 \lambda_5\right) v^2 - \frac{1}{\sqrt{2}} \frac{c_H^2}{s_H} \mu_1 v - 3\sqrt{2} s_H \mu_2 v, \end{aligned} \tag{2.22}$$

$$\begin{aligned} m_{H_3}^2 &\equiv m_{H_3^+}^2 = m_{H_3^0}^2 \\ &= -\frac{1}{2}\lambda_5 v^2 - \frac{1}{\sqrt{2} s_H} \mu_1 v, \end{aligned} \tag{2.23}$$

$$\begin{aligned} m_{H_1}^2 &\equiv m_{H_1^0}^2 \\ &= M_{11}^2 s_\alpha^2 + M_{22}^2 c_\alpha^2 - 2M_{12}^2 s_\alpha c_\alpha \\ &= \frac{1}{2}\left[M_{11}^2 + M_{22}^2 + \sqrt{(M_{11}^2 - M_{22}^2)^2 + 4(M_{12}^2)^2}\right], \end{aligned} \tag{2.24}$$

$$\begin{aligned} m_h^2 &= M_{11}^2 c_\alpha^2 + M_{22}^2 s_\alpha^2 + 2M_{12}^2 s_\alpha c_\alpha \\ &= \frac{1}{2}\left[M_{11}^2 + M_{22}^2 - \sqrt{(M_{11}^2 - M_{22}^2)^2 + 4(M_{12}^2)^2}\right]. \end{aligned} \tag{2.25}$$

Due to the custodial symmetry, physical Higgs bosons in the same $SU(2)_V$ multiplet have the degenerated mass at the tree level. It is a straightforward task to express the five dimensionless parameters $\lambda_1, \ldots, \lambda_5$ in terms of the physical Higgs boson masses $m_{H_5}, m_{H_3}, m_{H_1}, m_h$ and the mixing angle α [14]. To implement the GM model in GRACE, all the particles should be given in their mass eigenstates and interaction vertices are written in these states with physical parameters. We choose a set of independent physical parameters originating from the Higgs potential as follows: the 4 physical Higgs boson masses $(m_{H_5}, m_{H_3}, m_{H_1}, m_h)$, the VEV v and the 2 mixing angles (θ_H and α) and the 2 dimensionful trilinear couplings (μ_1 and μ_2).

The isospin doublet field $\phi = (\phi^+, \phi^0)$ has the Yukawa interactions with quarks and leptons:

$$\mathcal{L}_Y = -\overline{Q'_L} Y_u \tilde{\phi} u'_R - \overline{Q'_L} Y_d \phi d'_R - \overline{L'_L} Y_e \phi e'_R + \text{h.c.}, \quad (2.26)$$

where $\tilde{\phi} = i\tau^2 \phi^*$ and the fermion fields with primes are in the weak-eigenstate basis. Neglecting Majorana neutrino masses, which arise from the Yukawa interactions between the complex isospin triplet χ and the lepton doublets, one finds the Yukawa interactions in the GM model having the following form for every generations in the mass-eigenstate basis:

$$\begin{aligned}\mathcal{L}_Y \supset & -\sum_{f=u,d,e} \frac{m_f}{v} \left[\frac{c_\alpha}{c_H} \bar{f} f h - \frac{s_\alpha}{c_H} \bar{f} f H_1^0 \right. \\ & \left. + i \text{Sign}(f) t_H \bar{f} \gamma_5 f H_3^0 \right] \\ & + \left\{ -\frac{\sqrt{2} V_{ud}}{v} t_H \bar{u} (m_u \mathcal{P}_L - m_d \mathcal{P}_R) d H_3^+ \right. \\ & \left. + \frac{\sqrt{2} m_e}{v} t_H \bar{\nu} \mathcal{P}_R e H_3^+ + \text{h.c.} \right\}. \end{aligned} \quad (2.27)$$

Here V_{ud} is an appropriate element of the Cabibbo–Kobayashi–Maskawa matrix, the projection operator is defined as $\mathcal{P}_{R,L} = (1 \pm \gamma_5)/2$ and $\text{Sign}(f)$ is given by

$$\text{Sign}(f) = \begin{cases} +1 & \text{for } f = u, \\ -1 & \text{for } f = d, e. \end{cases} \quad (2.28)$$

Note that the custodial 5-plet Higgs bosons (H_5^{++}, H_5^+, H_5^0 in Eqs. (2.11), (2.12) and (2.14)) are linear combinations of the component fields in the isospin triplets ξ and χ. Therefore, they do not have the usual Yukawa interactions with fermions as in the SM and become fermiophobic.

3 Extension of the GRACE system

The GRACE system is a set of programs for automatic calculation of invariant amplitudes in quantum field theory developed by the Minami-Tateya collaboration at KEK. The user can obtain numerical results of various cross sections and decay widths by selecting the appropriate phase space option. The public version of GRACE can perform calculations in the SM and the minimal supersymmetric standard model [8,9]. This system can be extended by adding particles and interactions to a few text files describing the model-dependent part as appropriate. For example, an extension to the two-Higgs-doublet model and an analysis using it was done in Ref. [42].

We extended GRACE for the SM to perform calculations in the GM model. Specifically, we incorporated the set of Higgs particles ($H_5^{\pm\pm}, H_5^\pm, H_5^0, H_3^\pm, H_3^0, H_1^0, h^0$) and their interactions with gauge bosons and fermions.[3] We selected the following 30 types of two-body decay widths and $2 \to 2$ cross sections, and systematically tested the correctness of these incorporations by checking whether the analytical results and GRACE results agree by at least 10 orders of magnitude.

$$H_5^{++} \to W^+ W^+, \quad W^+ H_3^+, \quad (3.1)$$
$$H_5^+ \to W^+ Z, \quad Z H_3^+, \quad W^+ H_3^0, \quad (3.2)$$
$$H_5^0 \to W^+ W^-, \quad ZZ, \quad Z H_3^0, \quad W^+ H_3^-, \quad (3.3)$$
$$H_3^+ \to t\bar{b}, \quad c\bar{s}, \quad W^+ H_1^0, \quad W^+ h^0, \quad (3.4)$$
$$H_3^0 \to t\bar{t}, \quad b\bar{b}, \quad Z H_1^0, \quad Z h^0, \quad (3.5)$$
$$H_1^0 \to t\bar{t}, \quad b\bar{b}, \quad W^+ W^-, \quad ZZ, \quad (3.6)$$
$$h^0 \to b\bar{b}, \quad (3.7)$$
$$e^+ e^- \to H_5^{++} H_5^{--}, \quad H_5^+ H_5^-, \quad H_3^+ H_3^-, \quad Z h^0, \quad (3.8)$$
$$e^+ \nu_e \to H_5^{++} H_5^-, \quad H_5^+ H_5^0, \quad H_3^+ H_3^0, \quad W^+ h^0. \quad (3.9)$$

Formulae for cross sections and decay widths used in the analytical calculations, as well as expressions for the interaction coefficients, are provided in Appendix A.

In addition, we have reproduced the production cross sections of several Higgs bosons at e^+e^- colliders that are shown in Fig. 5 of Ref. [15]. The list of concrete processes is as follows:

$$e^+ e^- \to H_5^{++} H_5^{--}, \quad H_5^+ H_5^-, \quad (3.10)$$
$$e^+ e^- \to Z H_5^0, \quad W^- H_5^+ + \text{c.c.}, \quad W^- W^- H_5^{++} + \text{c.c.}, \quad (3.11)$$
$$e^+ e^- \to e^- \bar{\nu}_e H_5^+ + \text{c.c.}, \quad \nu_e \bar{\nu}_e H_5^0, \quad e^+ e^- H_5^0. \quad (3.12)$$

Typical Feynman diagrams contributing to these processes are shown in Fig. 1. The first type includes pair production of the doubly- and singly-charged Higgs bosons. The second and third types involve vector boson associated (VBA) and vector boson fusion (VBF) processes, respectively. One can also find calculations for these production cross sections in Ref. [13].

The GRACE model files for the GM model are available from the authors upon request.

4 Numerical results

In this section, we present production cross sections of the custodial 5-plet Higgs bosons at future e^+e^- and e^-e^- colliders, computed by using GRACE implementing the GM

[3] Three- and four-scalar vertices are not needed for the numerical results presented in the next section. We leave implementation of such interaction vertices and analysis that can be affected by them for future work.

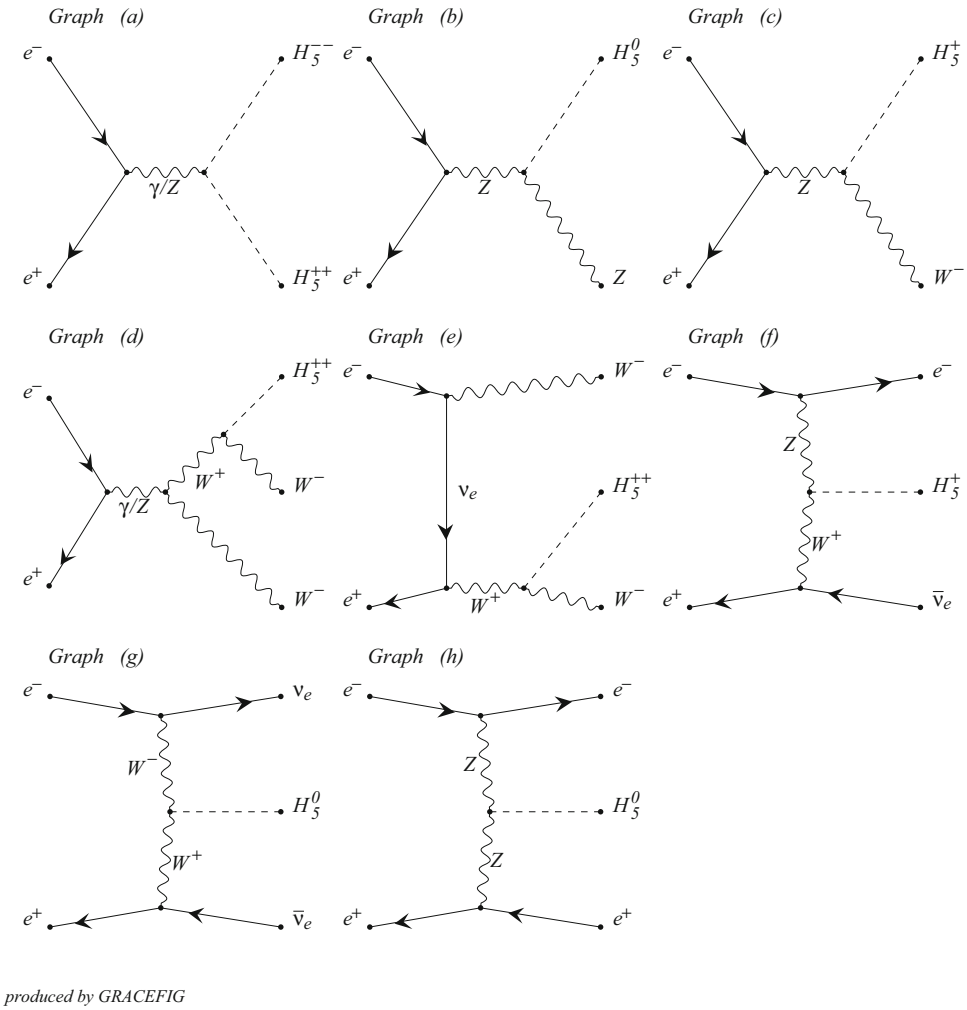

Fig. 1 Typical Feynman diagrams for the 5-plet Higgs boson production in e^+e^- collisions: **a** $e^+e^- \to H_5^{++}H_5^{--}$ (similar diagrams for $e^+e^- \to H_5^+H_5^-$), **b** $e^+e^- \to ZH_5^0H_5^0$, **c** $e^+e^- \to W^-H_5^+$, **d**, **e** $e^+e^- \to W^-W^-H_5^{++}$, **f** $e^+e^- \to e^-\bar{\nu}_e H_5^+$, **g** $e^+e^- \to \nu_e\bar{\nu}_e H_5^0$ and **h** $e^+e^- \to e^+e^-H_5^0$. The diagram (**a**) is classified as pair production, the diagrams (**b**)–(**e**) are VBA type, and the diagrams (**f**)–(**h**) are VBF type

model. The center-of-mass energy $\sqrt{s}$ is assumed to be 0.5 TeV. Typical Feynman diagrams appearing in e^-e^- processes we consider are shown in Fig. 2. Among the unknown model parameters in the GM model, only the 5-plet Higgs boson mass m_{H_5} and the doublet-triplet mixing angle θ_H affects these cross sections. The latest CMS result [40] excludes $s_H \equiv \sin\theta_H = 2\sqrt{2}v_\Delta/v$ greater than 0.20–0.35 at the 95% confidence level for a wide range of m_{H_5}. On the other hand, some points of $m_{H_5} \lessapprox 140\,\text{GeV}$ in the full parameter space are already excluded by Drell–Yan production of H_5^0 decaying to diphoton [39]. Therefore, as a typical benchmark point, we take $v_\Delta = 10\,\text{GeV}$ ($s_H \approx 0.11$) with varying m_{H_5} from 150 GeV to around $\sqrt{s}$. In addition to the above experimental constraints, these points satisfy the theoretical constraints in Ref. [14].

Figure 3 shows the mass m_{H_5} dependence of the total cross section for several neutral H_5^0 particle production processes in e^+e^- and e^-e^- collisions. Here, $e^+e^- \to ZH_5^0$ has only a VBA-type Feynman diagram, except negligible ones. The other e^+e^- processes contain Feynman diagrams of both VBA and VBF types, but for a comparison purpose the results here are restricted to the VBF type only. The curves for $e^+e^- \to \nu_e\bar{\nu}_e H_5^0$ and $e^+e^- \to e^+e^-H_5^0$ are due to WW fusion and ZZ fusion, respectively. The difference in the magnitude of the interaction coefficient is reflected in the difference in the cross sections. The reader should bear in mind that, as mentioned above, these two e^+e^- processes also have Feynman diagrams of the VBA type (via $e^+e^- \to ZH_5^0$ and the subsequent Z decay), thus for phenomenological purposes such contributions need to be taken into account.

In Fig. 3, we have also plotted the curve for $e^-e^- \to e^-e^-H_5^0$, which originally has contributions only from the Feynman diagrams of VBF type. In fact, we can see that the size of this cross section is almost the same as $e^+e^- \to e^+e^-H_5^0$ except for the VBA type; the tiny deviation comes from the fact that the e^-e^- scattering has two diagrams where one is the crossed diagram of the other and the interference of the two diagrams gives a tiny but positive contribution. In both processes, once the integral luminosity of $L = 10\,\text{ab}^{-1}$ is accumulated, more than a few tens of events can be expected in the search for neutral H_5^0 particles with mass less than about 350 GeV. However, it is necessary to evaluate the background events to determine whether the search is actually possible or not.

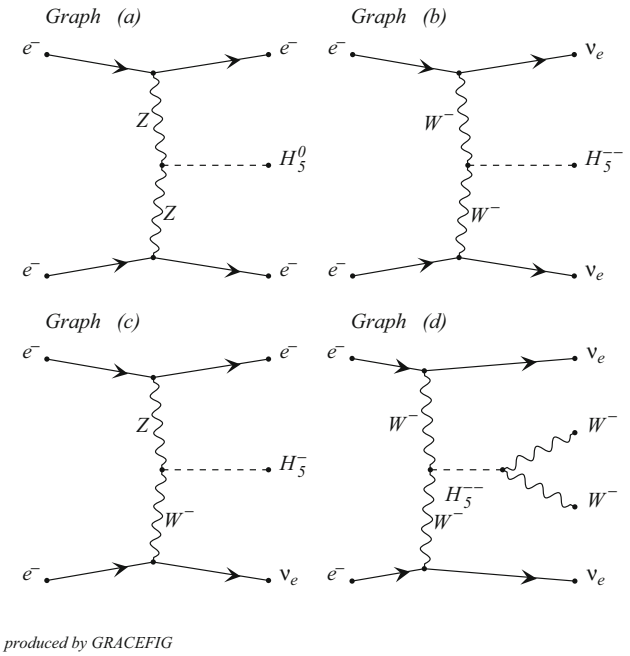

Fig. 2 Typical Feynman diagrams contributing to: **a** $e^-e^- \to e^-e^-H_5^0$, **b** $e^-e^- \to \nu_e\nu_e H_5^{--}$, **c** $e^-e^- \to e\nu_e H_5^-$ and **d** $e^-e^- \to \nu_e\nu_e W^-W^-$

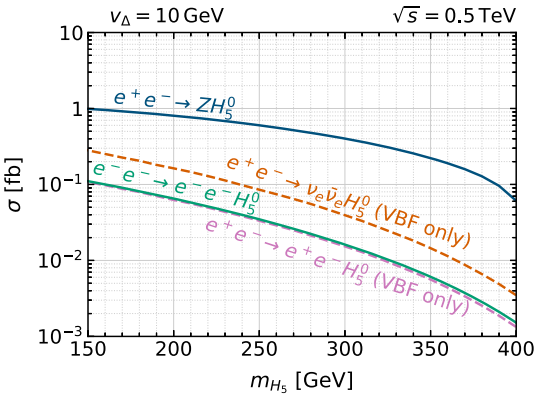

Fig. 3 The H_5^0 production cross sections at e^+e^- and e^-e^- colliders. For the dashed curves ($e^+e^- \to \nu_e\bar{\nu}_e H_5^0$ and $e^+e^- \to e^+e^-H_5^0$), only VBF-type diagrams are taken into account in the computations

Now let us turn our attention to scattering processes in e^-e^- collisions caused entirely by the VBF-type diagrams. Figure 4 shows the production cross sections of neutral, singly- and doubly-charged H_5 particles at e^-e^- colliders. Since these particles are produced with a similar phase space as the VBF type, the difference in the size of the cross sections is more or less a simple dependence on the interaction constants. The ratios of the cross sections in Fig. 4 read $\sigma(e^-e^- \to \nu_e\nu_e H_5^{--})/\sigma(e^-e^- \to e^-\nu_e H_5^-) = 3.2$–$3.8$ and $\sigma(e^-e^- \to e^-\nu_e H_5^-)/\sigma(e^-e^- \to e^-e^-H_5^0) = 4.8$–$5.2$, and both of them gradually increase as $m_{H_5}/\sqrt{s}$ does. These numbers are fairly close to 3 and 9/2, respectively,

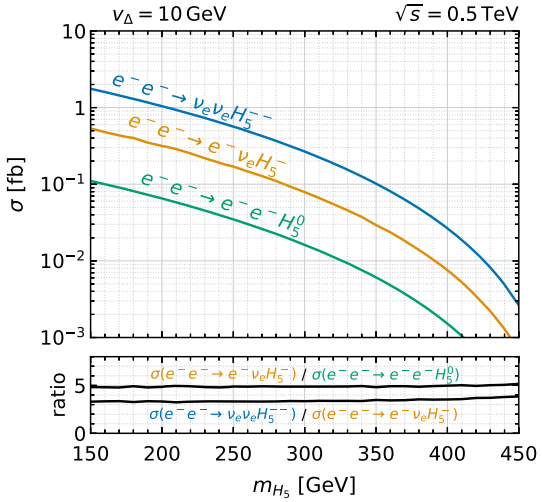

Fig. 4 The 5-plet Higgs boson production cross sections at e^-e^- colliders. The ratios of the cross sections are also plotted at the bottom

which can be obtained by using a VBF cross-section formula in the high energy limit $\sqrt{s} \to \infty$, see Appendix B. If such a ratio of the production cross sections is confirmed experimentally, then it would suggest the possibility of the H_5 Higgs boson group in the GM model, and therefore could be useful information for model verification. We emphasize that such simplicity of single 5-plet Higgs boson production processes in e^-e^- collisions is because they contain only VBF-type contributions. Single production processes in e^+e^- collisions have more complicated mass m_{H_5} dependence due to the VBA type besides the VBF type.

Since neutral or singly-charged extra Higgs bosons are predicted by many extended Higgs models, we now turn to the doubly-charged H_5^{--} particle distinctive to the GM model. Figure 5 shows the calculated production cross sections of the doubly-charged H_5^{--} particle in e^+e^- and e^-e^- collisions. Here, in the computation for $e^+e^- \to W^+W^+H_5^{--}$ + c.c., we have omitted Feynman diagrams containing the pair production $e^+e^- \to H_5^{++}H_5^{--}$ with the subsequent decay $H_5^{++} \to W^+W^+$; the calculation included only the remaining diagrams, all of which are classified as the VBA-type diagrams. There are two targets to search for H_5^{--} particles in e^+e^- collisions: pair production and single production. The cross section of the pair production is useful because of its large value due to the fact that it is determined only by the gauge couplings [13,15] and does not depend on s_H that is now rather constrained experimentally. This is a distinctive feature of the pair production; all the other production cross sections plotted in Figs. 3, 4 and 5 are suppressed by s_H^2. However, the accessible mass value in the pair production is limited to $\sqrt{s}/2$. On the other hand, since the single production of H_5^{--} in e^+e^- collisions involves a W^+W^+ pair, the upper limit of the search mass range is $\sqrt{s} - 2m_W$; there is no significant extension

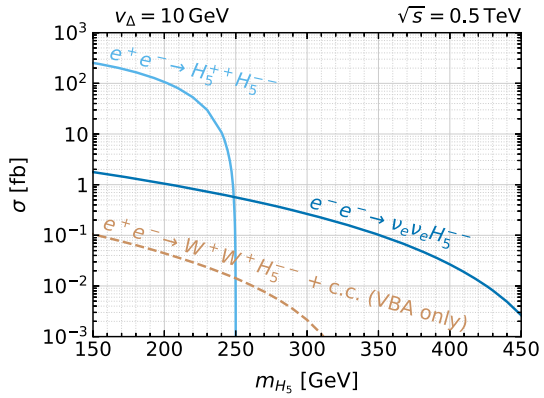

Fig. 5 The doubly-charged 5-plet Higgs boson production cross sections at e^+e^- and e^-e^- colliders. The dashed curve ($e^+e^- \to W^+W^+H_5^{--}$ + c.c.) is obtained by considering only the VBA-type diagrams

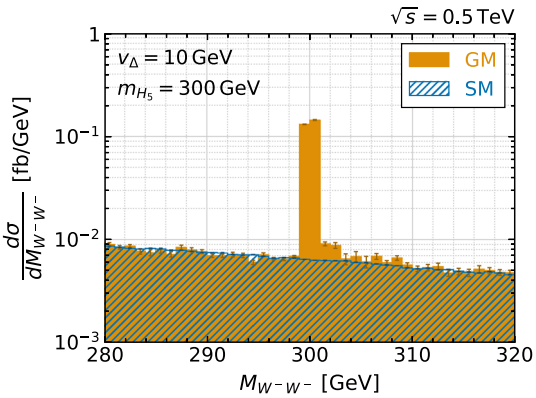

Fig. 6 The W^-W^- invariant mass distribution for $e^-e^- \to \nu_e\nu_e W^-W^-$. Each error bar indicates the statistical error of the Monte Carlo integration for each bin

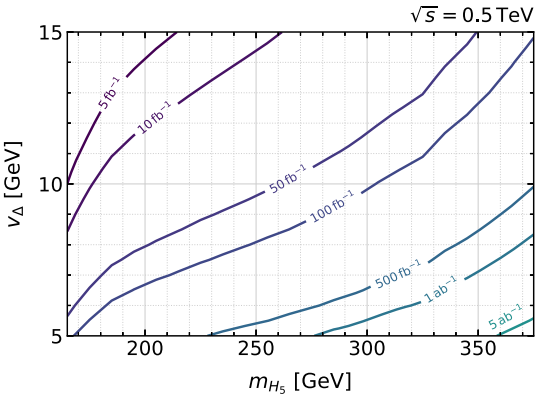

Fig. 7 The integrated luminosity required for a 5-σ discovery by the W^-W^- invariant mass distribution for $e^-e^- \to \nu_e\nu_e W^-W^-$. A common invariant mass window cut $m_{H_5} - 20\,\text{GeV} \le M_{W^-W^-} \le m_{H_5} + 20\,\text{GeV}$ is used for every m_{H_5} and $\text{BR}(H_5^{--} \to W^-W^-) = 1$ is assumed

in comparison with the pair production for a moderate value of $\sqrt{s}$. By contrast, in e^-e^- collisions, there is a process $e^-e^- \to \nu_e\nu_e H_5^{--}$ that has a wider search mass range. Specifically, in this process, the search range is extended to $m_{H_5} \sim \sqrt{s}$ in principle. In fact, we can see from Fig. 5 that about 100 events are expected for $L = 10\,\text{ab}^{-1}$ of integrated luminosity when $m_{H_5} \sim 0.4\,\text{TeV}$ with $\sqrt{s} = 0.5\,\text{TeV}$. Note that the cross section for $e^-e^- \to \nu_e\nu_e H_5^{--}$ in Fig. 5 is more than 6 times larger than that for $e^+e^- \to \nu_e\bar{\nu}_e H_5^0$ (VBF only) in Fig. 3; the difference between them comes entirely from that in the Higgs couplings to two W bosons, except in the interference term in the former.

If the H_5^{--} particle decays mainly into a W^-W^- pair, then we expect to observe a resonance peak at $M_{W^-W^-} \sim m_{H_5}$ in the invariant mass $M_{W^-W^-}$ distribution of W^- pairs in the $e^-e^- \to \nu_e\nu_e W^-W^-$ process (see the resonant diagram Fig. 2d). In Fig. 6, we plot the $M_{W^-W^-}$ distribution with $m_{H_5} = 300\,\text{GeV}$ for that decay branching ratio of 100%,[4] along with the contribution from the SM. Admittedly, a similar plot was obtained in Ref. [17], but here we update the plot considering the current experimental constraints.

Note that, unlike hadron colliders such as the LHC and LHeC [44], the invariant mass $M_{W^-W^-}$ can be cleanly reconstructed using the 4-jets from $W^- \to q\bar{q}'$ decays in the e^-e^- collider. The total cross section of the W^- pair with missing energy in the SM is about 2.5 fb, whereas the total cross section of the signal in the GM model is about 2.8 fb. From this result, it is clear that if we simply consider only the statistical error in the value of the total cross section and the number of events,[5] an integral luminosity of about $1\,\text{ab}^{-1}$ is required to obtain an event excess of $5\,\sigma$, while about 100fb^{-1} is sufficient when the analysis is limited to the region of Fig. 6. We also show a contour plot in the m_{H_5}-v_Δ plane, in Fig. 7, for the integrated luminosity required for a 5-σ discovery via a signal in the W^-W^- invariant mass distribution of $e^-e^- \to \nu_e\nu_e W^-W^-$. For this plot, we have used a common invariant mass window cut $m_{H_5} - 20\,\text{GeV} \le M_{W^-W^-} \le m_{H_5} + 20\,\text{GeV}$ for every m_{H_5} and assumed all H_5^{--} decay into W^-W^- pairs.

Considering how to search for the 5-plet Higgs bosons in the GM model using VBF processes at future linear colliders, especially via the WW fusion processes because of their relatively large sizes of the cross sections, one immediately sees the following fact: due to the electric charges,

[4] $\text{BR}(H_5^{\pm\pm} \to W^\pm W^\pm) \approx 1$ is usually assumed in analyses for the LHC [43], which is true if $\Delta m \equiv m_{H_5} - m_{H_3}$ is smaller than m_W. For $\Delta m > m_W$, the decay branching ratio of $H_5^{--} \to W^-H_3^-$ is no longer zero. The details of the signal in this case are currently under analysis. In general, the result depends on m_{H_3} and the mixing angle α (if a subsequent $H_3^- \to hW^-$ decay is considered), and is beyond the scope of this paper, thus will be presented elsewhere.

[5] For simplicity, we use $Z = S/\sqrt{B}$ as an estimator to compute the signal significance Z, where S and B are the numbers of signal and background events, respectively.

e^+e^- colliders can produce the H_5^0 bosons in this channel, while e^-e^- colliders produce the H_5^{--} bosons. Therefore, a search strategy can be developed as follows. With a future linear collider running under an e^+e^- mode, we first target the H_5^0 boson by using $e^+e^- \to H_5^0 +$ invisible with a subsequent H_5^0 decay into a W^+W^- or ZZ pair, assuming $\mathrm{BR}(H_5^0 \to VV) \approx 1$. If found, then this will be certainly an outstanding triumph, but countless models are predicting such a new neutral scalar particle. Then, suppose the linear collider has an e^-e^- mode as an option. We next run the collider under the e^-e^- mode in order to target the H_5^{--} boson by using $e^-e^- \to H_5^{--} +$ invisible with a subsequent H_5^{--} decay into a W^-W^- pair. If nature adopts the GM model and the discovered extra neutral Higgs boson is indeed H_5^0, then we will find a resonant peak by H_5^{--} at the same mass, strongly suggesting that the model may be correct. This will hopefully be further confirmed by the search for H_5^- in e^-e^- collisions.

5 Summary

We have discussed our extension of the GRACE system to perform calculations in the Georgi–Machacek (GM) model. After a systematic check of the implemented set of model files against the known results of the $1 \to 2$ and $2 \to 2$ processes, we have analyzed the fermiophobic custodial 5-plet Higgs boson production processes in the GM model at e^+e^- and e^-e^- colliders with the center-of-mass energy of $\sqrt{s} = 0.5$ TeV. The mass of m_{H_5} and the triplet VEV v_Δ have been chosen as typical values that are not currently ruled out by the experimental data.

The neutral 5-plet Higgs boson H_5^0 can be produced in several processes both at e^+e^- and e^-e^- colliders, provided $m_{H_5} < \sqrt{s}$. As shown in Fig. 3, the largest cross section is obtained for $e^+e^- \to ZH_5^0$. The other processes have smaller cross sections, however, even the ZZ fusion processes possibly lead to enough events to be detected with the integrated luminosity expected at future colliders. We have also pointed out that at e^-e^- colliders the sizes of the neutral, singly- and doubly-charged 5-plet Higgs boson production cross sections via vector boson fusions have a relatively simple dependence of coupling constants. The ratios of the cross sections are fairly close to those estimated in the high energy limit even at $\sqrt{s} = 0.5$ TeV.

Since the doubly-charged Higgs boson $H_5^{\pm\pm}$ is one of the characteristic particles in the GM model, we have performed computations for its production, for which e^-e^- colliders are rather suitable from the viewpoint of the quantum number of the initial state. While the $H_5^{++}H_5^{--}$ pair production at e^+e^- colliders can be used for searches with the mass of m_{H_5} only up to $\sqrt{s}/2$, the single H_5^{--} production at e^-e^- colliders can reach heavier mass regions. We have also investigated the resonant $M_{W^-W^-}$ distribution in $e^-e^- \to \nu_e\nu_e W^-W^-$ with an assumption that the decay branching ratio for $H_5^{--} \to W^-W^-$ is 100%.

In this paper, we have focused on the 5-plet Higgs boson production, but one can also consider 3-plet and singlet Higgs boson production at e^-e^- colliders. We leave it for future work.

Acknowledgements We are grateful to Takuto Nagura for discussions and for his participation in this study at the early stage. The work by T.U. is in part supported by JSPS KAKENHI Grant numbers 19K03831 and 21K03583.

Data Availability Statement This manuscript has no associated data or the data will not be deposited. [Authors' comment: This is a theoretical study and no experimental data.]

Funded by SCOAP[3].

Appendix A: Formulae

In the following formulae we use variables $x_A \equiv m_A^2/M_H^2$, $z_A \equiv m_A^2/s$ and the function $\lambda(x, y) \equiv 1 + x^2 + y^2 - 2x - 2y - 2xy$. N_c is the color factor of the final state fermions.

- Decay widths for $H \to VV'$, $H \to H'V$ and $H \to f\bar{f}'$

$$\Gamma(H \to VV') = \frac{g_{HVV'}^2}{8\pi M_H}\lambda^{\frac{1}{2}}(x_V, x_{V'}) \times \left[1 + \frac{(1 - x_V - x_{V'})^2}{8x_V x_{V'}}\right], \tag{A.1}$$

$$\Gamma(H \to H'V) = \frac{g_{HH'V}^2}{16\pi} M_H \lambda^{\frac{1}{2}}(x_{H'}, x_V) \times \left[\frac{(1 - x_{H'} + x_V)^2}{x_V} - 4\right], \tag{A.2}$$

$$\Gamma(H \to f\bar{f}') = \frac{N_c}{16\pi} M_H \lambda^{\frac{1}{2}}\left(x_f, x_{f'}\right) \times \left[\left(\left|g_{Hff'}^L\right|^2 + \left|g_{Hff'}^R\right|^2\right)(1 - x_f - x_{f'}) - 4\Re\left(g_{Hff'}^L g_{Hff'}^{R*}\right)\sqrt{x_f x_{f'}}\right]. \tag{A.3}$$

- Differential cross sections for $f\bar{f}' \to HH'$
  - $(f, \bar{f}') = (e^-_{L,R}, e^+)$ and $(H, H') = (H_5^{++}, H_5^{--})$, (H_5^+, H_5^-), (H_3^+, H_3^-)

$$\frac{d\sigma_{L,R}}{d\cos\theta} = \frac{\lambda^{\frac{3}{2}}(z_H, z_{H'})}{64\pi s} \times \left(g_{HH'\gamma} g_{ff'\gamma} + \frac{g_{HH'Z} g^{L,R}_{ff'Z}}{1 - z_Z} \right)^2 \sin^2\theta. \quad \text{(A.4)}$$

  - $(f, \bar{f}') = (\nu_{eL}, e^+)$ and $(H, H') = (H_5^{++}, H_5^-)$, (H_5^+, H_5^0), (H_3^+, H_3^0)

$$\frac{d\sigma_{L}}{d\cos\theta} = \frac{\lambda^{\frac{3}{2}}(z_H, z_{H'})}{32\pi s} \times \left(\frac{g_{HH'W} g^{L}_{ff'W}}{1 - z_W} \right)^2 \sin^2\theta. \quad \text{(A.5)}$$

- Differential cross sections for $f\bar{f}' \to Vh^0$
  - $(f, \bar{f}') = (e^-_{L,R}, e^+)$ and $V = Z$

$$\frac{d\sigma_{L,R}}{d\cos\theta} = \frac{\lambda^{\frac{1}{2}}(z_V, z_h)}{64\pi s^2} \left(\frac{g_{hVV} g^{L,R}_{ff'V}}{1 - z_V} \right)^2 \left[2 + \frac{\lambda(z_V, z_h)}{4 z_V} \sin^2\theta \right]. \quad \text{(A.6)}$$

  - Equation (A.6) can be applied also for $(f, \bar{f}') = (\nu_{eL}, e^+)$ and $V = W^+$, but then an extra factor 2 must be multiplied.

- Coupling constants

$$g_{H_5^{\pm\pm} W^\mp W^\mp} = \frac{g^2}{\sqrt{2}} s_H v, \quad \text{(A.7)}$$

$$g_{H_5^{\pm} W^\mp Z} = \mp \frac{g g_Z}{2} s_H v, \quad \text{(A.8)}$$

$$g_{H_5^0 W^+ W^-} = -\frac{g^2}{2\sqrt{3}} s_H v, \quad \text{(A.9)}$$

$$g_{H_5^0 ZZ} = \frac{g_Z^2}{\sqrt{3}} s_H v, \quad \text{(A.10)}$$

$$g_{H_1^0 W^+ W^-} = -\frac{g^2}{6} \left(3 s_\alpha c_H - 2\sqrt{6} c_\alpha s_H \right) v, \quad \text{(A.11)}$$

$$g_{H_1^0 ZZ} = -\frac{g_Z^2}{6} \left(3 s_\alpha c_H - 2\sqrt{6} c_\alpha s_H \right) v, \quad \text{(A.12)}$$

$$g_{h^0 W^+ W^-} = \frac{g^2}{6} \left(3 c_\alpha c_H + 2\sqrt{6} s_\alpha s_H \right) v, \quad \text{(A.13)}$$

$$g_{h^0 ZZ} = \frac{g_Z^2}{6} \left(3 c_\alpha c_H + 2\sqrt{6} s_\alpha s_H \right) v, \quad \text{(A.14)}$$

$$g_{H_5^{++} H_5^{--} \gamma} = 2e, \quad \text{(A.15)}$$

$$g_{H_5^{+} H_5^{-} \gamma} = -e, \quad \text{(A.16)}$$

$$g_{H_3^{+} H_3^{-} \gamma} = -e, \quad \text{(A.17)}$$

$$g_{H_5^{++} H_5^{--} Z} = g_Z \left(1 - 2 s_W^2 \right), \quad \text{(A.18)}$$

$$g_{H_5^{+} H_5^{-} Z} = -\frac{g_Z}{2} \left(1 - 2 s_W^2 \right), \quad \text{(A.19)}$$

$$g_{H_3^{+} H_3^{-} Z} = -\frac{g_Z}{2} \left(1 - 2 s_W^2 \right), \quad \text{(A.20)}$$

$$g_{H_5^{\pm} H_3^{\mp} Z} = \pm \frac{g_Z}{2} c_H, \quad \text{(A.21)}$$

$$g_{H_5^0 H_3^0 Z} = i \frac{g_Z}{\sqrt{3}} c_H, \quad \text{(A.22)}$$

$$g_{H_3^0 H_1^0 Z} = -i \frac{g_Z}{6} \left(3 s_\alpha s_H + 2\sqrt{6} c_\alpha c_H \right), \quad \text{(A.23)}$$

$$g_{H_5^{\pm\pm} H_5^{\mp} W^\mp} = -\frac{g}{\sqrt{2}}, \quad \text{(A.24)}$$

$$g_{H_5^{\pm} H_5^0 W^\mp} = \frac{\sqrt{3}}{2} g, \quad \text{(A.25)}$$

$$g_{H_5^{\pm\pm} H_3^{\mp} W^\mp} = -\frac{g}{\sqrt{2}} c_H, \quad \text{(A.26)}$$

$$g_{H_5^{\pm} H_3^0 W^\mp} = \mp i \frac{g}{2} c_H, \quad \text{(A.27)}$$

$$g_{H_3^{\pm} H_5^0 W^\mp} = -\frac{g}{2\sqrt{3}} c_H, \quad \text{(A.28)}$$

$$g_{H_3^{\pm} H_3^0 W^\mp} = \mp i \frac{g}{2}, \quad \text{(A.29)}$$

$$g_{H_3^{\pm} H_1^0 W^\mp} = \frac{g}{6} \left(3 s_\alpha s_H + 2\sqrt{6} c_\alpha c_H \right), \quad \text{(A.30)}$$

$$g_{H_3^{\pm} h^0 W^\mp} = -\frac{g}{6} \left(3 c_\alpha s_H - 2\sqrt{6} s_\alpha c_H \right), \quad \text{(A.31)}$$

$$g_{H_3^0 h^0 Z} = i \frac{g_Z}{6} \left(3 c_\alpha s_H - 2\sqrt{6} s_\alpha c_H \right), \quad \text{(A.32)}$$

$$g^L_{H_3^{+,-} ud} = -\sqrt{2} V_{ud} \frac{m_{u,d}}{v} t_H, \quad \text{(A.33)}$$

$$g^R_{H_3^{+,-} ud} = \sqrt{2} V_{ud} \frac{m_{d,u}}{v} t_H, \quad \text{(A.34)}$$

$$g^R_{H_3^{+} ev} = \sqrt{2} \frac{m_e}{v} t_H, \quad \text{(A.35)}$$

$$g^L_{H_3^{-} ev} = \sqrt{2} \frac{m_e}{v} t_H, \quad \text{(A.36)}$$

$$g^L_{H_3^0 uu} = i \frac{m_u}{v} t_H, \quad \text{(A.37)}$$

$$g^R_{H_3^0 uu} = -i \frac{m_u}{v} t_H, \quad \text{(A.38)}$$

$$g^L_{H_3^0 dd} = -i \frac{m_d}{v} t_H, \quad \text{(A.39)}$$

$$g^R_{H_3^0 dd} = i \frac{m_d}{v} t_H, \quad \text{(A.40)}$$

$$g^L_{H_3^0 ee} = -i \frac{m_e}{v} t_H, \quad \text{(A.41)}$$

$$g^R_{H_3^0 ee} = i \frac{m_e}{v} t_H, \quad \text{(A.42)}$$

$$g^{L,R}_{H_1^0 uu} = \frac{m_u}{v} \frac{s_\alpha}{c_H}, \quad \text{(A.43)}$$

$$g^{L,R}_{H_1^0 dd} = \frac{m_d}{v} \frac{s_\alpha}{c_H}, \quad \text{(A.44)}$$

$$g^{L,R}_{H^0_1 ee} = \frac{m_e}{v}\frac{s_\alpha}{c_H}, \tag{A.45}$$

$$g^{L,R}_{h^0 uu} = -\frac{m_u}{v}\frac{c_\alpha}{c_H}, \tag{A.46}$$

$$g^{L,R}_{h^0 dd} = -\frac{m_d}{v}\frac{c_\alpha}{c_H}, \tag{A.47}$$

$$g^{L,R}_{h^0 ee} = -\frac{m_e}{v}\frac{c_\alpha}{c_H}. \tag{A.48}$$

Here, we have used additional shorthand notations $g_Z = g/\cos\theta_W$ and $s_W = \sin\theta_W$.

Appendix B: Ratios of VBF total cross sections

The typical Feynman diagram contribution for VBF processes can be written as, in the Feynman gauge,

$$\mathcal{M}_A = i g_{V_1 V_2 H} \frac{\left[\bar{u}(p_3)\gamma^\mu (g_{R_1}\mathcal{P}_R + g_{L_1}\mathcal{P}_L)u(p_1)\right]\left[\bar{u}(p_4)\gamma_\mu (g_{R_2}\mathcal{P}_R + g_{L_2}\mathcal{P}_L)u(p_2)\right]}{\left[(p_1-p_3)^2 - m^2_{V_1}\right]\left[(p_2-p_4)^2 - m^2_{V_2}\right]}. \tag{B.1}$$

Here, an incoming fermion with the momentum p_1 splits into a fermion with the momentum p_3 and the gauge boson of mass m_{V_1} via the interaction specified by g_{R_1} and g_{L_1}. The same for the other side; namely, the other incoming fermion with the momentum p_2 splits into a fermion with the momentum p_4 and the gauge boson of mass m_{V_2} via the interaction specified by g_{R_2} and g_{L_2}. The Higgs boson of mass m_H is produced by the fusion of the two gauge bosons with the coupling $g_{V_1 V_2 H}$. All fermion masses are ignored.

For e^-e^- collisions, one should also consider a crossed diagram, obtained by the exchange of the incoming electrons, $\mathcal{M}_B = -(\mathcal{M}_A \text{ with } p_1 \leftrightarrow p_2)$. One can argue that the interference term between $\mathcal{M}_A$ and $\mathcal{M}_B$ is negligible [45].[6] If one is interested only in the total cross section, $|\mathcal{M}_B|^2$ gives the same contribution as $|\mathcal{M}_A|^2$, thus a factor 2 is multiplied.

As a crude approximation in the high energy limit ($\sqrt{s} \gg m_H, m_{V_1}, m_{V_2}$), one can drive a Weizsäcker–Williams-type expression for the total cross section [47–50].[7] The result for e^-e^- collisions is

$$\sigma \simeq \frac{\mathcal{S} g^2_{V_1 V_2 H} C}{2(4\pi)^3 m^2_{V_1} m^2_{V_2}}\left[(1+z_H)\ln\left(\frac{1}{z_H}\right) - 2 + 2z_H\right], \tag{B.2}$$

where $\mathcal{S}$ represents the statistical factor for the outgoing fermions, $z_H = m^2_H/s$ and

$$C = (g^2_{R_1} + g^2_{L_1})(g^2_{R_2} + g^2_{L_2}). \tag{B.3}$$

Although this formula overestimates the total cross section by a factor $\gtrapprox 2$ for $\sqrt{s} = 0.5$ TeV, one may expect that such deviations cancel for the most part when ratios are taken. With this formula, the ratios of the VBF cross sections at e^-e^- colliders presented in Sect. 4 are estimated as

$$\frac{\sigma(e^-e^- \to \nu_e \nu_e H_5^{--})}{\sigma(e^-e^- \to e^-\nu_e H_5^-)} \simeq 2\left(\frac{\cos^2\theta_W}{1 - 4\sin^2\theta_W + 8\sin^4\theta_W}\right) \approx 3, \tag{B.4}$$

$$\frac{\sigma(e^-e^- \to e^-\nu_e H_5^-)}{\sigma(e^-e^- \to e^-e^- H_5^0)} \simeq 3\left(\frac{\cos^2\theta_W}{1 - 4\sin^2\theta_W + 8\sin^4\theta_W}\right) \approx \frac{9}{2}. \tag{B.5}$$

Note that the couplings between H_5 and two vector bosons arise from the kinetic term of the isospin triplet, picking up the triplet VEV. Thus, all of them are proportional to $s_H v$, resulting in the above ratios consisting of group theoretical factors and the weak mixing angle. In general, if one considers other ratios, e.g., of production cross sections of H_5 and H_1, then the other mixing angle α appears as well as θ_H.

[6] In fact, this was numerically observed in Ref. [46] for $e^-e^- \to e^-e^- ZZ \to e^-e^- h$ in the SM. See also the almost negligible deviation between the two curves for the ZZ fusion at e^+e^- and e^-e^- colliders in Fig. 3 and its explanation in the text.

[7] The leading logarithmic term was obtained in Ref. [51], which is indeed sufficient to obtain the ratios in Eqs. (B.4) and (B.5). The approximation can be in principle improved by eliminating kinematical oversimplifications, see, e.g., Ref. [52].

References

1. ATLAS collaboration, Observation of a new particle in the search for the Standard Model Higgs boson with the ATLAS detector at the LHC. Phys. Lett. B **716**, 1 (2012). https://doi.org/10.1016/j.physletb.2012.08.020. arXiv:1207.7214 [hep-ex]
2. CMS collaboration, Observation of a new boson at a mass of 125 GeV with the CMS experiment at the LHC. Phys. Lett. B **716**, 30 (2012). https://doi.org/10.1016/j.physletb.2012.08.021. arXiv:1207.7235 [hep-ex]
3. I.P. Ivanov, Building and testing models with extended Higgs sectors. Prog. Part. Nucl. Phys. **95**, 160 (2017). https://doi.org/10.1016/j.ppnp.2017.03.001 arXiv:1702.03776 [hep-ph]
4. S. Dawson, C. Englert, T. Plehn, Higgs physics: it ain't over till it's over. Phys. Rep. **816**, 1 (2019). https://doi.org/10.1016/j.physrep.2019.05.001 arXiv:1808.01324 [hep-ph]
5. K. Hartling, K. Kumar, H.E. Logan, GMCALC: a calculator for the Georgi–Machacek model. arXiv:1412.7387 [hep-ph]
6. S. Kanemura, M. Kikuchi, K. Mawatari, K. Sakurai, K. Yagyu, H-COUP Version 2: a program for one-loop corrected Higgs boson decays in non-minimal Higgs sectors. Comput. Phys. Commun. **257** (2020). https://doi.org/10.1016/j.cpc.2020.107512. arXiv:1910.12769 [hep-ph]
7. D. Fontes, J.C. Romão, FeynMaster: a plethora of Feynman tools. Comput. Phys. Commun. **256** (2020). https://doi.org/10.1016/j.cpc.2020.107311. arXiv:1909.05876 [hep-ph]

8. F. Yuasa et al., Automatic computation of cross-sections in HEP: status of GRACE system. Prog. Theor. Phys. Suppl. **138**, 18 (2000). https://doi.org/10.1143/PTPS.138.18 arXiv:hep-ph/0007053
9. J. Fujimoto et al., GRACE/SUSY automatic generation of tree amplitudes in the minimal supersymmetric standard model. Comput. Phys. Commun. **153**, 106 (2003). https://doi.org/10.1016/S0010-4655(03)00159-0 arXiv:hep-ph/0208036
10. Minami-Tateya Collaboration, GRACE version 2.2.1. http://www.minami-home.kek.jp/
11. H. Georgi, M. Machacek, Doubly charged Higgs bosons. Nucl. Phys. B **262**, 463 (1985). https://doi.org/10.1016/0550-3213(85)90325-6
12. M.S. Chanowitz, M. Golden, Higgs boson triplets with $M_W = M_Z \cos\theta_W$. Phys. Lett. B **165**, 105 (1985). https://doi.org/10.1016/0370-2693(85)90700-2
13. J.F. Gunion, R. Vega, J. Wudka, Higgs triplets in the standard model. Phys. Rev. D **42**, 1673 (1990). https://doi.org/10.1103/PhysRevD.42.1673
14. C.-W. Chiang, K. Yagyu, Testing the custodial symmetry in the Higgs sector of the Georgi–Machacek model. JHEP **01**, 026 (2013). https://doi.org/10.1007/JHEP01(2013)026 arXiv:1211.2658 [hep-ph]
15. C.-W. Chiang, S. Kanemura, K. Yagyu, Phenomenology of the Georgi–Machacek model at future electron–positron colliders. Phys. Rev. D **93**, 055002 (2016). https://doi.org/10.1103/PhysRevD.93.055002 arXiv:1510.06297 [hep-ph]
16. T.G. Rizzo, Inverse neutrinoless double beta decay. Phys. Lett. B **116**, 23 (1982). https://doi.org/10.1016/0370-2693(82)90027-2
17. V.D. Barger, J.F. Beacom, K. Cheung, T. Han, Production of weak bosons and Higgs bosons in e^-e^- collisions. Phys. Rev. D **50**, 6704 (1994). https://doi.org/10.1103/PhysRevD.50.6704 arXiv:hep-ph/9404335
18. CMS Collaboration, Observation of electroweak production of same-sign W boson pairs in the two jet and two same-sign lepton final state in proton-proton collisions at $\sqrt{s} = 13$ TeV. Phys. Rev. Lett. **120**, 081801 (2018). https://doi.org/10.1103/PhysRevLett.120.081801. arXiv:1709.05822 [hep-ex]
19. ATLAS Collaboration, Observation of electroweak production of a same-sign W boson pair in association with two jets in pp collisions at $\sqrt{s} = 13$ TeV with the ATLAS detector. Phys. Rev. Lett. **123**, 161801 (2019). https://doi.org/10.1103/PhysRevLett.123.161801. arXiv:1906.03203 [hep-ex]
20. J.L. Feng, Physics at e^-e^- colliders. Mod. Phys. A **15**, 2355 (2000). https://doi.org/10.1142/S0217751X0000242XInt.J arXiv:hep-ph/0002055
21. T.P. Cheng, L.-F. Li, Neutrino masses, mixings and oscillations in SU(2) × U(1) models of electroweak interactions. Phys. Rev. D **22**, 2860 (1980). https://doi.org/10.1103/PhysRevD.22.2860
22. J. Schechter, J.W.F. Valle, Neutrino masses in SU(2) × U(1) theories. Phys. Rev. D **22**, 2227 (1980). https://doi.org/10.1103/PhysRevD.22.2227
23. M. Magg, C. Wetterich, Neutrino mass problem and gauge hierarchy. Phys. Lett. B **94**, 61 (1980). https://doi.org/10.1016/0370-2693(80)90825-4
24. G. Lazarides, Q. Shafi, C. Wetterich, Proton lifetime and fermion masses in an SO(10) model. Nucl. Phys. B **181**, 287 (1981). https://doi.org/10.1016/0550-3213(81)90354-0
25. R.N. Mohapatra, G. Senjanovic, Neutrino masses and mixings in gauge models with spontaneous parity violation. Phys. Rev. D **23**, 165 (1981). https://doi.org/10.1103/PhysRevD.23.165
26. J.F. Gunion, R. Vega, J. Wudka, Naturalness problems for $\rho = 1$ and other large one loop effects for a standard model Higgs sector containing triplet fields. Phys. Rev. D **43**, 2322 (1991). https://doi.org/10.1103/PhysRevD.43.2322
27. H.E. Logan, M.-A. Roy, Higgs couplings in a model with triplets. Phys. Rev. D **82**, 115011 (2010). https://doi.org/10.1103/PhysRevD.82.115011 arXiv:1008.4869 [hep-ph]
28. ATLAS Collaboration, Combined measurements of Higgs boson production and decay using up to 80 fb^{-1} of proton–proton collision data at $\sqrt{s} = 13$ TeV collected with the ATLAS experiment. Phys. Rev. D **101**, 012002 (2020). https://doi.org/10.1103/PhysRevD.101.012002. arXiv:1909.02845 [hep-ex]
29. CMS Collaboration, Combined measurements of Higgs boson couplings in proton–proton collisions at $\sqrt{s} = 13$ TeV. Eur. Phys. J. C **79**, 421 (2019). https://doi.org/10.1140/epjc/s10052-019-6909-y. arXiv:1809.10733 [hep-ex]
30. C.-W. Chiang, T. Yamada, Electroweak phase transition in Georgi–Machacek model. Phys. Lett. B **735**, 295 (2014). https://doi.org/10.1016/j.physletb.2014.06.048 arXiv:1404.5182 [hep-ph]
31. R. Zhou, W. Cheng, X. Deng, L. Bian, Y. Wu, Electroweak phase transition and Higgs phenomenology in the Georgi–Machacek model. JHEP **01**, 216 (2019). https://doi.org/10.1007/JHEP01(2019)216 arXiv:1812.06217 [hep-ph]
32. M. Aoki, S. Kanemura, Unitarity bounds in the Higgs model including triplet fields with custodial symmetry. Phys. Rev. D **77**, 095009 (2008). https://doi.org/10.1103/PhysRevD.77.095009. arXiv:0712.4053 [hep-ph] [Erratum https://doi.org/10.1103/PhysRevD.89.059902 ibid.**89** (2014) 059902]
33. K. Hartling, K. Kumar, H.E. Logan, The decoupling limit in the Georgi–Machacek model. Phys. Rev. D **90**, 015007 (2014). https://doi.org/10.1103/PhysRevD.90.015007 arXiv:1404.2640 [hep-ph]
34. M.E. Krauss, F. Staub, Perturbativity constraints in BSM models. Eur. Phys. J. C **78**, 185 (2018). https://doi.org/10.1140/epjc/s10052-018-5676-5 arXiv:1709.03501 [hep-ph]
35. M.E. Krauss, F. Staub, Unitarity constraints in triplet extensions beyond the large s limit. Phys. Rev. D **98**, 015041 (2018). https://doi.org/10.1103/PhysRevD.98.015041 arXiv:1805.07309 [hep-ph]
36. B. Li, Z.-L. Han, Y. Liao, Higgs production at future e^+e^- colliders in the Georgi–Machacek model. JHEP **02**, 007 (2018). https://doi.org/10.1007/JHEP02(2018)007 arXiv:1710.00184 [hep-ph]
37. C.-W. Chiang, G. Cottin, O. Eberhardt, Global fits in the Georgi–Machacek model. Phys. Rev. D **99**, 015001 (2019). https://doi.org/10.1103/PhysRevD.99.015001 arXiv:1807.10660 [hep-ph]
38. N. Ghosh, S. Ghosh, I. Saha, Charged Higgs boson searches in the Georgi–Machacek model at the LHC. Phys. Rev. D **101**, 015029 (2020). https://doi.org/10.1103/PhysRevD.101.015029 arXiv:1908.00396 [hep-ph]
39. A. Ismail, H.E. Logan, Y. Wu, Updated constraints on the Georgi–Machacek model from LHC Run 2. arXiv:2003.02272 [hep-ph]
40. CMS Collaboration, Search for charged Higgs bosons produced in vector boson fusion processes and decaying into vector boson pairs in proton–proton collisions at $\sqrt{s} = 13$ TeV. Eur. Phys. J. C **81**, 723 (2021). https://doi.org/10.1140/epjc/s10052-021-09472-3. arXiv:2104.04762 [hep-ex]
41. D. Das, I. Saha, Cornering variants of the Georgi–Machacek model using Higgs precision data. Phys. Rev. D **98**, 095010 (2018). https://doi.org/10.1103/PhysRevD.98.095010 arXiv:1811.00979 [hep-ph]
42. T. Kon, T. Nagura, T. Ueda, K. Yagyu, Double Higgs boson production at e^+e^- colliders in the two-Higgs-doublet model. Phys. Rev. D **99**, 095027 (2019). https://doi.org/10.1103/PhysRevD.99.095027 arXiv:1812.09843 [hep-ph]
43. M. Zaro, H. Logan, Recommendations for the interpretation of LHC searches for H_5^0, $H_5^\pm$, and $H_5^{\pm\pm}$ in vector boson fusion with decays to vector boson pairs, LHCHXSWG-2015-001 (2015)
44. H. Sun, X. Luo, W. Wei, T. Liu, Searching for the doubly-charged Higgs bosons in the Georgi–Machacek model at the electron–proton colliders. Phys. Rev. D **96**, 095003 (2017). https://doi.org/10.1103/PhysRevD.96.095003 arXiv:1710.06284 [hep-ph]

45. D.A. Dicus, S.S.D. Willenbrock, Higgs bosons from vector boson fusion in e^+e^-, ep and pp collisions. Phys. Rev. D **32**, 1642 (1985). https://doi.org/10.1103/PhysRevD.32.1642
46. K. Hikasa, Heavy Higgs production in e^+e^- and e^-e^- collisions. Phys. Lett. B **164**, 385 (1985). https://doi.org/10.1016/0370-2693(85)90346-6 [Erratum https://doi.org/10.1016/0370-2693(87)91584-X ibid.**195** (1987) 623]
47. G.L. Kane, W.W. Repko, W.B. Rolnick, The effective $W^{\pm}$, Z^0 approximation for high-energy collisions. Phys. Lett. B **148**, 367 (1984). https://doi.org/10.1016/0370-2693(84)90105-9
48. M.S. Chanowitz, M.K. Gaillard, The TeV physics of strongly interacting W's and Z's. Nucl. Phys. B **261**, 379 (1985). https://doi.org/10.1016/0550-3213(85)90580-2
49. S. Dawson, The effective W approximation. Nucl. Phys. B **249**, 42 (1985). https://doi.org/10.1016/0550-3213(85)90038-0
50. G. Altarelli, B. Mele, F. Pitolli, Heavy Higgs production at future colliders. Nucl. Phys. B **287**, 205 (1987). https://doi.org/10.1016/0550-3213(87)90103-9
51. R.N. Cahn, S. Dawson, Production of very massive Higgs bosons. Phys. Lett. B **136**, 196 (1984). https://doi.org/10.1016/0370-2693(84)91180-8 [Erratum https://doi.org/10.1016/0370-2693(84)91941-5 ibid. **138** (1984) 464]
52. P.W. Johnson, F.I. Olness, W.-K. Tung, The effective vector boson method for high-energy collisions. Phys. Rev. D **36**, 291 (1987). https://doi.org/10.1103/PhysRevD.36.291